Sager, W.W., Kanazawa, T., and Escutia, C. (Eds.)
Proceedings of the Ocean Drilling Program, Scientific Results Volume 191

7. Paleomagnetism of Basaltic Rocks Cored at ODP Site 1179: Implications for Mid-Cretaceous Pacific Plate Paleolatitude and Paleomagnetic Pole[1]

William W. Sager[2] and Benjamin C. Horner-Johnson[3]

ABSTRACT

During Ocean Drilling Program Leg 191, ~100 m of mid-Cretaceous igneous crust was cored at Site 1179 (41.08°N, 159.96°E), located within magnetic Anomaly M8 on the abyssal plain of the northwest Pacific Ocean near Shatsky Rise. Paleomagnetic data from this section are significant because they can constrain the mid-Cretaceous Pacific plate paleolatitude and paleomagnetic pole, both of which can be used to infer tectonic drift and other geodynamic processes. In this study, we analyzed the paleomagnetism of 122 samples from 40 flows in the Site 1179 basalt section. Comparison of inclination data among flows implies 13 independent measurements of the paleomagnetic field. Assuming a reversed magnetic polarity because of the site location within Anomaly M8, the data give a mean paleocolatitude of 88.1° ± 6.8° (corresponding to a paleolatitude of 1.9°N). The paleocolatitude is consistent with other mid-Cretaceous Pacific paleomagnetic data that indicate ~39° northward drift of the western Pacific plate since mid-Cretaceous time. Comparison of observed between-flow colatitude variance with that expected from secular variation data suggests that secular variation may not have been completely averaged with the 13 independent groups sampled at Site 1179. Colatitude scatter in the section is markedly less in the deepest 33 m of the hole, indicating a shift

[1]Sager, W.W., and Horner-Johnson, B.C., 2004. Paleomagnetism of basaltic rocks cored at ODP Site 1179: implications for mid-Cretaceous Pacific plate paleolatitude and paleomagnetic pole. *In* Sager, W.W., Kanazawa, T., and Escutia, C. (Eds.), *Proc. ODP, Sci. Results,* 191, 1–20 [Online]. Available from World Wide Web: <http://www-odp.tamu.edu/publications/191_SR/VOLUME/CHAPTERS/002.PDF>. [Cited YYYY-MM-DD]
[2]Department of Oceanography, Texas A&M University, 317A Eller Building, College Station TX 77843-3146, USA. **wsager@ocean.tamu.edu**
[3]Department of Earth Science, Rice University, 6100 South Main Street, Houston TX 77005, USA.

Initial receipt: 23 July 2003
Acceptance: 19 August 2003
Web publication: 9 March 2004
Ms 191SR-002

from rapidly erupted flows in the bottom ~33 m of the section to more slowly emplaced flows above.

INTRODUCTION

Paleomagnetic measurements from oceanic basaltic rock cores are important for tectonic studies because they give site paleolatitude and can be used to trace past plate motions. Such data are especially significant for Pacific plate studies because the plate is almost entirely covered with water, so few traditional paleomagnetic data are available. Moreover, Pacific paleomagnetic data are desirable for global tectonic studies as a result of the plate's rapid motion, large area, and unparalleled record of drift relative to the hotspots.

Because fully oriented paleomagnetic data from outcrops are rare, the apparent polar wander path (APWP) for the Pacific plate is mostly constrained by data from cores, analyses of magnetic lineation asymmetry (skewness), and inversions of magnetic anomalies over seamounts (e.g., Gordon, 1983; Cox and Gordon, 1984; Sager and Pringle, 1988; Petronotis and Gordon, 1999; Sager and Koppers, 2000). Limitations for each of these data types make interpretation and synthesis of an APWP more challenging.

Seamount magnetic anomaly inversions are the most abundant data, but may suffer the most systematic bias (e.g., Sager et al., 1993). Seamount paleomagnetic poles are calculated with the assumption that the anomaly results from a magnetization that was entirely acquired at the time of formation and is homogeneous throughout the seamount. Although these are adequate approximations for many seamounts, neither assumption is likely to be strictly true (Sager et al., 1993). The result is scatter in paleomagnetic pole positions caused by magnetization inhomogeneities and a shift of the pole toward or away from the present geomagnetic pole (depending on seamount polarity), resulting from the contribution from induced or viscous magnetization (Sager et al., 1993; Sager and Koppers, 2000). Accurate dating of seamounts is also problematic; consequently, only a small number of seamount paleopoles are useful for APWP determination (Sager and Koppers, 2000).

Paleopoles calculated from lineation skewness data are fewer in number but provide greater time resolution because the Cretaceous and Cenozoic magnetic reversal timescale is relatively well dated. Skewness data cannot be determined for the Cretaceous Long Normal Superchron, so there is a gap of ~35 m.y. during the mid-Cretaceous for which no skewness poles can be determined. In addition, skewness data suffer from a systematic error, known as "anomalous skewness," the source of which is still unclear (Cande, 1978; Petronotis et al., 1992). With coeval anomalies from two or more different lineation sets, anomalous skewness can be estimated with the assumption that this factor is constant for anomalies of the same age (Larson and Sager, 1992; Petronotis et al., 1992). Although this may reduce the bias caused by anomalous skewness, there are poorly understood differences in pole positions estimated from skewness data and other data types (e.g., Petronotis et al., 1994).

Many paleomagnetic measurements have been made on Deep Sea Drilling Program (DSDP) and Ocean Drilling Program (ODP) cores taken from the Pacific plate. These data also have limitations imposed by acquisition and geologic factors. Virtually all such data give only the mag-

netic inclination because the coring tool rotates around a vertical axis and azimuthal orientation of the core is rarely possible. This lack of azimuthal orientation results in a lack of magnetic declination data, and as a result only the paleolatitude of the site can be determined (Peirce, 1976; Cox and Gordon, 1984). Thus, determination of a paleopole usually requires combining coeval paleolatitude data from widely separated sites (Peirce, 1976; Cox and Gordon, 1984).

An additional problem for sedimentary core paleomagnetic data is that the fidelity of the paleoinclination may be in doubt (Gordon, 1990; Tarduno, 1990). Although many sediment core paleolatitude data are consistent with coeval paleomagnetic data (Peirce, 1976; Sager and Pringle, 1988), some display a systematic error termed "inclination shallowing." This bias appears to be caused by compaction or the adherence of magnetic particles to clay particles, and its result is to cast doubt on the accuracy of sedimentary core paleomagnetic data.

Basalt flows are thought to be reliable magnetic field recorders if enough flows can be sampled to average secular variation. Unfortunately, few DSDP and ODP holes have penetrated more than several meters into basaltic basement, so few sites have sufficient data to do so. Even when numerous flows are sampled, secular variation averaging may be in doubt because multiple flows can be extruded in a short time and therefore not all flows are independent measurements of the magnetic field. One of the deepest basalt sections was drilled from Hole 433C into the top of Suiko Seamount. This section recovered 65 flows, which produced only ~20–30 groups considered magnetically independent (Kono, 1980; Cox and Gordon, 1984). Although paleolatitudes have been determined with fewer numbers of units, the results may have large uncertainties because of insufficient averaging (Cox and Gordon, 1984; Sager, 2002). Nevertheless, even imprecise paleolatitude data are important because basalt core paleolatitudes can be combined with coeval data and weighted according to their uncertainties to calculate paleopoles (Gordon and Cox, 1980; Cox and Gordon, 1984).

During Leg 191, Hole 1179D (41.08°N, 159.96°E) was bored ~100 m into basaltic rocks located on the abyssal plain northwest of Shatsky Rise (Fig. F1). Because the hole is located on magnetic Anomaly M8 (Shipboard Scientific Party, 2001), the implied age of the igneous crust is ~129 Ma using the geomagnetic polarity reversal timescale (Gradstein et al., 1994). Coring recovered 49.9 m of mostly fresh, aphyric basalt flows and pillows, comprising 48 flow units divided by changes in texture, composition, or cooling boundaries (Shipboard Scientific Party, 2001). Igneous units in the sequence were grouped into three sections based on the abundance of olivine: (1) Group I, olivine-poor basalt (flows 1–8; 367.9–396.4 meters below seafloor [mbsf]); (2) Group II, olivine-free basalt (flows 8–24; 396.4–438.8 mbsf); and (3) Group III, olivine-rich basalt (flows 24–48; 438.8–471.4 mbsf). With 48 igneous flow units cored, the Site 1179 basalts provide an excellent opportunity to determine an Early Cretaceous paleolatitude for the Pacific plate. Here we report a study of the paleomagnetic characteristics of this igneous section, determine a paleolatitude, and discuss tectonic implications. Because of the location of Site 1179 on Anomaly M8 (the source of which is a block of reversed polarity crust), we expected the basalt sample magnetization to be reversed polarity. Other paleomagnetic studies from the western Pacific indicate that the Pacific plate has drifted 30°–40° northward since the mid-Cretaceous, so we expected that the Site 1179 crust was emplaced slightly north of the equator. Our results are consistent with these hypotheses.

F1. Location of Site 1179 relative to Shatsky Rise, p. 12.

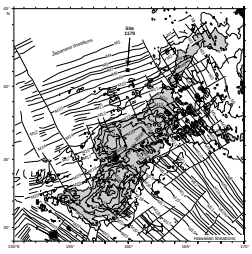

METHODS AND ANALYSIS

A total of 122 samples were measured in this study (Table T1). Samples were obtained as 2.5-cm (1 in) minicores drilled perpendicular to the vertical split face of the rock cores. Samples were taken only from hemicylindrical pieces long enough to ensure that they remained vertically oriented during rotary coring. An upcore orientation mark was scribed on each sample to provide a vertical reference. Samples were spaced at irregular intervals in the core, depending on recovery, unit boundaries, and physical state of core pieces, with the object of collecting at least two to three samples from each lava flow (the range of samples per flow is 1 to 8). Eight flows were not sampled owing to the lack of suitably oriented pieces (Table T1).

T1. Basalt sample paleomagnetic data, p. 17.

Samples were measured with the shipboard direct-current superconducting quantum interference device (DC-SQUID) cryogenic magnetometer onboard *JOIDES Resolution*. All samples were demagnetized to isolate a characteristic remanent magnetization. Both alternating field (AF) and thermal demagnetization methods were applied to a subset of samples to assess the efficacy of each method. Results from the thermal treatment appeared to better isolate a characteristic remanence than those from AF demagnetization, so thermal demagnetization was used for most samples (Table T1). A total of 101 samples were studied with thermal demagnetization, and the remaining 21 samples were studied with AF demagnetization. Stepwise thermal demagnetization was typically conducted beginning at 150°C and continuing in 50°C steps up to 450°–625°C. On occasion additional measurements were made with 25°C steps above 400° to 450°C. Usually the AF demagnetization proceeded in 5-mT steps from 10–40 or 50 mT and 10-mT steps up to 70 mT, but a few experiments included smaller demagnetization steps.

Demagnetization results from each sample were plotted on an orthogonal vector diagram to aid in finding a characteristic magnetization direction. Using principal component analysis (Kirschvink, 1980), a least-squares line was fit to a straight segment of the demagnetization curve that trended toward the plot origin. The best least-squares magnetization vector was calculated, along with the maximum angle of deflection (MAD) (Kirschvink, 1980), a measure of the scatter in the points constraining the magnetization inversion (Table T1). Characteristic magnetization directions and MAD angles were calculated for each sample using two principal component analysis methods, one with the demagnetization vector tied to the origin and one with the vector free to assume any angle. Although the latter usually produced larger MAD angles, it was preferred because its assumptions were not as restrictive and the results were more consistent. In most cases the difference in direction between the two methods was small (<5°).

Magnetization inclinations from the individual samples were combined to calculate a mean paleolatitude for the site in several steps. We used analysis methods described by Cox and Gordon (1984), which recommend working with colatitude rather than inclination, but are otherwise similar to inclination analysis. First, colatitude values for samples from each individual flow were averaged to determine a flow mean. In several flows, one or two sample measurements were significantly different from other samples in the same flow (typically >2 σ from the mean of the other samples) and those measurements were not used in calculating the flow average. In two other flows, approximately equal numbers of samples had different signs, requiring reinterpretation of

the flow divisions (see below). Flow average colatitude values were tested against those of adjacent flows to see if they were statistically different at the 95% confidence level using the Z-statistic (Kono, 1980). If adjacent means were not statistically distinct, they were combined and the procedure repeated with other adjacent flows. Using this method, a series of statistically distinct flow group means was calculated.

Cox and Gordon (1984) recommend that flow group means be averaged if they represent a time interval less than the coherency time of paleosecular variation so that there is no bias from a time interval that is more heavily sampled. To accomplish this, we judged group means to be serially correlated if they did not show a large change between successive means (~10°) or if a group of colatitudes followed a smooth trend (Cox and Gordon, 1984). Although this procedure is subjective, the result is a more conservative estimate of the number of independent flow mean colatitudes. In addition, the mean colatitude and uncertainty estimates are not greatly affected by differences among the selection of correlated units.

Independent group mean colatitude values (Table T2) and an average colatitude (Table T3) were computed following the methods of Cox and Gordon (1984). This procedure both provides a correction for bias caused by averaging inclination-only data and gives an estimate of the data errors and site mean colatitude. An estimate of the random error is determined from between-group colatitude variations, and an estimate of the colatitude variance produced by secular variation is taken from a model of secular variation data. The final error bounds are calculated including an assumed systematic error of 2° that can be caused by off-vertical tilt of the borehole (a quantity not measured during Leg 191) and correcting for the number of independent group means (Cox and Gordon, 1984).

T2. Paleomagnetic unit averaging results, p. 19.

T3. Mean colatitude statistics, p. 20.

RESULTS

Most samples displayed univectorial decay toward the origin of an orthogonal vector plot with little or moderate scatter in direction between successive demagnetization steps (Figs. F2, F3). A total of 89 (73%) samples gave MAD angles of <10° (Table T1), implying well-determined characteristic magnetization vectors. It was typically possible to use five to six demagnetization steps (range = 3–9) to define the characteristic remanence direction (Table T1), another indication of demagnetization consistency. Only eight samples were so erratic that they gave MAD angles >30°. Most of these samples are present in flows 7 and 8, suggesting a link to flow characteristics.

A steep, downward-directed overprint, like that often attributed to an isothermal remanent magnetization (IRM) imparted by the drill string (e.g., Roberts et al., 1996), was present in many samples. This overprint was usually removed by thermal demagnetization of >100°–300°C or AF demagnetization in fields >15–25 mT. Many samples treated with AF demagnetization did not show decay toward the orthogonal vector plot origin at high field steps (Fig. F2), a behavior that probably results from an anhysteretic remanent magnetization (ARM) imparted by imperfectly balanced AF demagnetization coils. These samples were useful nevertheless because they typically displayed univectorial decay toward the plot origin at lower field values, which were used to determine the characteristic magnetization direction.

F2. AF demagnetization experiments, p. 13.

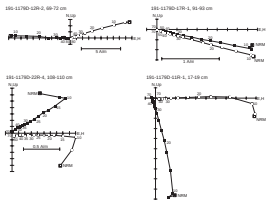

F3. Thermal demagnetization experiments, p. 14.

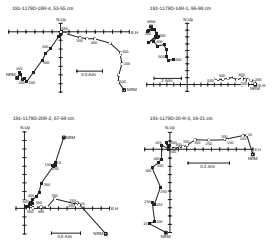

Orthogonal vector plots show that characteristic magnetization directions usually have small inclination values (Figs. F2, F3; Table T1), consistent with formation of the basalt section near the equator. Negative inclinations were measured from 95 samples (78%), implying that most of the section records an upward-directed magnetization. Positive inclination samples were sometimes grouped (as in flows 3, 8, 9, 11, and 21), and sometimes solitary. The solitary positive inclination data may result from inverted samples or erroneous inclinations. Single discordant samples were found in flows 9, 15, 20, 22, 24, and 45, whereas two discordant samples were found in flow 44 (Table T1). Because the source of the discrepancy is not known, these data were not used in averaging calculations. The groups of positive inclination values likely indicate flows with coherent downward-directed magnetizations. Although flows 3, 9, and 21 have predominantly positive inclination values, flows 8 and 11 each contain two groups of opposite sign but with equal numbers of samples (Table T1). Because the two groups in each of these flows show consistent inclinations, we think that the changes in sign are real and result from shipboard scientists failing to recognize a flow boundary. Thus flows 8 and 11 were each subdivided into two separate subunits (Table T1).

Combining data to calculate flow mean colatitudes produced 23 statistically distinct flow groups (Fig. F4). As a consequence of large interflow changes in colatitude above 400 mbsf, most flows above this depth appear to be independent units. In contrast, the lower section shows little variation and adjacent flow mean inclinations are often statistically distinct only as a result of low within-flow inclination scatter. Because flows 23–47 show little variation, we concluded they are serially correlated and their inclinations were averaged. This required us to ignore single inclination measurements from two flows (33 and 43) that appear to break the sequence. Although these flows may be independent units and represent actual breaks in the lava succession, with only one sample apiece the flow inclination values are not robust. We also ignored the single discordant inclination from flow 6 and averaged data from flows 5 and 7, which have similar means (Fig. F4; Table T1).

Averaging the 13 inclination groups yields a mean colatitude of 88.1° ± 6.8° (this and other error limits are 2 σ, approximating 95% confidence), assuming that the section is entirely reversed polarity and that the changes in inclination sign result from secular variation rather than polarity reversals. This paleocolatitude implies a paleolatitude of 1.9°N ± 6.8°. The average colatitude is not highly sensitive to the choice of flow groupings. For example, an average of all 23 statistically distinct flow groups yields a paleocolatitude of 87.5°.

F4. Measured colatitudes and flow mean colatitudes, p. 15.

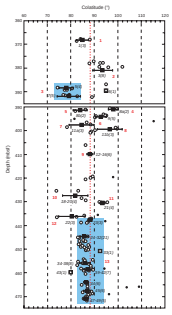

DISCUSSION

Several assumptions were made during the averaging of the paleomagnetic data that could change our results, so it is prudent to assess their impact. First, inclination values from 10 samples were not used in the flow averages (Table T1). These values were discarded because they appeared to be outliers when compared with other data from a given flow or flow group. They typically differed from the other samples in a given flow by >2 σ, frequently having an inclination sign opposite that of the other samples. It was not typical for such samples to display poor demagnetization consistency, so the discordant inclination values cannot be explained simply by samples with poor paleomagnetic character-

istics. Those samples with inclination absolute values similar to those of adjacent samples, but which show a difference in sign, may be explained as samples inverted during curation or handling of the cores. This explanation does not work for samples with greatly discordant inclinations, for example, Sample 191-1179D-12R-5, 14–16 cm, which gave an inclination of 52.7° despite a relatively low MAD value of 10.7° (Table T1). Such discordant results can occur when rock fragments fall from the borehole wall and are cored out of position and orientation. Discarding such errant points as outliers seems appropriate and is standard practice in paleomagnetic studies. Including the discordant measurements would not change the mean colatitude significantly but would unnecessarily enlarge the estimated error bounds.

Five flow groups that have samples with positive inclinations were assumed to be measurements of the same reversed polarity field as the other flow groups rather than polarity reversals. At higher paleolatitude sites, where there is little chance that secular variation would cause the difference in sign, flows that give an inclination with opposite sign are sometimes assumed to record a magnetic reversal. In contrast, at a low paleolatitude site changes in inclination sign caused by secular variation are expected. The latitude variance at the equator in models of secular variation based on paleomagnetic data is ~9° (Harrison, 1980; McElhinny and McFadden, 1997), far greater than the 1.9° average paleolatitude for Site 1179. In addition, the differences in sign are unlikely to result from overlapping lava flows of opposite polarities. Site 1179 is located near the middle of 37-km-wide Anomaly M8 (Shipboard Scientific Party, 2001), and because of the near 180° skewness of the magnetic lineations (Nakanishi et al., 1989; Larson and Sager, 1992) the anomaly is located directly over the reversed polarity source body. If the assumption that the entire section is reversed polarity is incorrect, the mean paleolatitude may be slightly greater. Changing the polarity of flow units with positive inclinations and reaveraging yields a mean paleocolatitude of 84.2°, a change of 4.1°. Furthermore, if the assumed polarity is incorrect, the implied normal polarity paleolatitude is 1.9°S.

Another subtle assumption made in averaging the data is that there is no overlap in cored flows, despite an apparent overlap of 2.6 m between the bottom of Core 191-1179D-12R and the top of 13R (Table T1). This discrepancy resulted from ODP core curation convention (which "expands" fractured hard rock core specimens) and the fact that Core 191-1179D-13R recovered 0.9 m more core than the estimated interval drilled. Although the cause of actual 0.9 m overlap between these two cores is unclear, it is doubtful that it could have been caused by drilling that resumed above the bottom of the hole (to cause overlap), so the assumption appears justified.

When calculating a paleocolatitude using a small number of independent measurements of the paleomagnetic field, the result may be inaccurate if secular variation is not properly averaged (Cox and Gordon, 1984). Despite the consistency of the Site 1179 colatitude with other mid-Cretaceous Pacific paleomagnetic data (Fig. F5), the statistics of our calculation suggest some uncertainty owing to insufficient secular variation averaging. We estimate that only 13 independent magnetic units were sampled, a number that would be considered inadequate to average secular variation in most paleomagnetic studies. Although the total colatitude variance is 14.6°, much of this scatter arises from measurement error and between-group colatitude variance is only 4.8°. This value is only half the expected 9.0° from secular variation models (Harrison, 1980; Cox and Gordon, 1984). This difference

F5. Comparison of Site 1179 paleocolatitude with other data, p. 16.

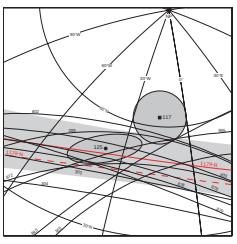

suggests that Site 1179 samples may not completely average secular variation. Nevertheless, because of the method used to determine the error bounds, which used an estimate of colatitude scatter from a secular variation model (Cox and Gordon, 1984), the calculated confidence limits are not biased by the lack of secular variation sampling.

Despite the cautions above, comparison of the Site 1179 paleocolatitude with other Pacific basalt core data of mid-Cretaceous age shows that our results are in good agreement (Fig. F5). The colatitude arc for the site goes through the middle of the distribution of other colatitude arcs of mid-Cretaceous age. Furthermore, the 125-Ma paleomagnetic pole calculated mainly from magnetic anomaly skewness (Petronotis and Gordon, 1999) falls within the error bounds of the colatitude.

The 1.8°N paleolatitude calculated from Site 1179 basalts implies that the site has drifted 39.3° northward since 129 Ma, a result consistent with other paleomagnetic data of similar age. Not only do other Pacific basalt cores (many with even fewer independent magnetic units) give similar results (Fig. F5), but the data are also consistent with seamount (Sager and Koppers, 2000) and skewness data (Larson et al., 1992; Petronotis and Gordon, 1999). This agreement suggests that the paleocolatitude is reliable.

In addition to the paleolatitude information, the Site 1179 basalt data also give some insight into the construction of the igneous section. Colatitude values from flows in the bottom part of the section show markedly less variation than those above, implying the lower section was emplaced rapidly, with little time between flows. The flows that exhibit little between-flow scatter, combined into unit 13 (Fig. F4), are those that belong to the distinct geochemical Group III, the olivine-rich flows (Shipboard Scientific Party, 2001). In contrast, flows in the upper part of the section exhibit large changes between successive flow groups, indicating significant time gaps. Along with the change in geochemistry (Shipboard Scientific Party, 2001), this may indicate a shift in the magma source or mode of flow emplacement.

CONCLUSIONS

Basalt samples from 40 flow units cored at Site 1179 were measured to yield characteristic magnetization inclinations and colatitude values. Flow average colatitudes were statistically compared, and those that were not distinct were combined and averaged. The result of our analysis is that the 40 flows represent only 13 independent measurements of the paleomagnetic field. A mean colatitude, 88.1° ± 6.8° was calculated, corrected for bias inherent in azimuthally unoriented samples. Assuming the section is reversed, as is consistent with drilling near the middle of Anomaly M8, the paleomagnetic data imply a paleolatitude of 1.9°N ± 6.8°. The Site 1179 paleocolatitude is consistent with other Pacific plate paleomagnetic data of similar age and indicates ~39° of northward drift of the western Pacific plate since the mid-Cretaceous. In addition, a shift in scatter between flow group colatitude values from low in the bottom ~33 m of the section to high in the upper section implies a change from rapid emplacement to longer time periods between successive flows.

ACKNOWLEDGMENTS

The authors thank Gary Acton and a cantankerous anonymous reviewer for valuable suggestions to improve the manuscript. This research used samples and data provided by the Ocean Drilling Program (ODP). The ODP is sponsored by the U.S. National Science Foundation (NSF) and participating countries under management of Joint Oceanographic Institutions (JOI) Inc. Funding for this research was provided a grant from JOI/U.S. Science Support Program (USSSP).

REFERENCES

Cande, S.C., 1978. Anomalous behavior of the paleomagnetic field inferred from the skewness of anomalies 33 and 34. *Earth Planet. Sci. Lett.,* 40:275–286.

Cox, A., and Gordon, R.G., 1984. Paleolatitudes determined from paleomagnetic data from vertical cores. *Rev. Geophys. Space Phys.,* 22:47–72.

Gordon, R.G., 1983. Late Cretaceous apparent polar wander of the Pacific plate: evidence for a rapid shift of the Pacific hotspots with respect to the spin axis. *Geophys. Res. Lett.,* 10:709–712.

————, 1990. Test for bias in paleomagnetically determined paleolatitudes from Pacific plate Deep Sea Drilling Project sediments. *J. Geophys. Res.,* 95:8397–8404.

Gordon, R.G., and Cox, A., 1980. Calculating paleomagnetic poles for oceanic plates. *Geophys. J. R. Astron. Soc.,* 63:619–640.

Gradstein, F.M., Agterberg, F.P., Ogg, J.G., Hardenbol, J., van Veen, P., Thierry, J., and Huang, Z., 1994. A Mesozoic time scale. *J. Geophys. Res.,* 99:24051–24074.

Hammond, S.R., Kroenke, L.W., and Theyer, F., 1975. Northward motion of the Ontong-Java Plateau between –110 and –30 m.y.: a paleomagnetic investigation of DSDP Site 289. *In* Andrews, J.E., and Packham, G., et al., *Init. Repts. DSDP,* 30: Washington (U.S. Govt. Printing Office) 415–418.

Harrison, C.G.A., 1980. Secular variation and excursions of the Earth's magnetic field. *J. Geophys. Res.,* 85:3511–3522.

Helsley, C.E., 1993. Paleomagnetic results from Leg 136. *In* Wilkens, R.H., Firth, J., Bender, J., et al., *Proc. ODP, Sci. Results,* 136: College Station, TX (Ocean Drilling Program), 45–50.

Kirschvink, J.L., 1980. The least-squares line and plane and the analysis of palaeomagnetic data. *Geophys. J. R. Astron. Soc.,* 62:699–718.

Kono, M., 1980. Paleomagnetism of DSDP Leg 55 basalts and implications for the tectonics of the Pacific plate. *In* Jackson, E.D., Koizumi, I., et al., *Init. Repts. DSDP,* 55: Washington (U.S. Govt. Printing Office), 737–752.

Larson, R.L., and Lowrie, W., 1975. Paleomagnetic evidence for motion of the Pacific plate from Leg 32 basalts and magnetic anomalies. *In* Larson, R.L., and Moberly, R., et al., *Init. Repts. DSDP,* 32: Washington (U.S. Govt. Printing Office), 571–577.

Larson, R.L., and Sager, W.W., 1992. Skewness of magnetic anomalies M0 to M29 in the northwestern Pacific. *In* Larson, R.L., Lancelot, Y., et al., *Proc. ODP, Sci. Results,* 129: College Station, TX (Ocean Drilling Program), 471–481.

Larson, R.L., Steiner, M.B., Erba, E., and Lancelot, Y., 1992. Paleolatitudes and tectonic reconstructions of the oldest portion of the Pacific plate: a comparative study. *In* Larson, R.L., Lancelot, Y., et al., *Proc. ODP, Sci. Results,* 129: College Station, TX (Ocean Drilling Program), 615–631.

McElhinny, M.W., and McFadden, P.L., 1997. Palaeosecular variation over the past 5 Myr based on a new generalized database. *Geophys. J. Int.,* 131:240–252.

Nakanishi, M., and Gee, J.S., 1995. Paleomagnetic investigations of volcanic rocks: paleolatitudes of the northwestern Pacific guyots. *In* Haggerty, J.A., Premoli Silva, I., Rack, F., and McNutt, M.K. (Eds.), *Proc. ODP, Sci. Results,* 144: College Station, TX (Ocean Drilling Program), 585–604.

Nakanishi, M., Sager, W.W., and Klaus, A., 1999. Magnetic lineations within Shatsky Rise, northwest Pacific Ocean: implications for hot spot–triple junction interaction and oceanic plateau formation. *J. Geophys. Res.,* 104:7539–7556.

Nakanishi, M., Tamaki, K., and Kobayashi, K., 1989. Mesozoic magnetic anomaly lineations and seafloor spreading history of the Northwestern Pacific. *J. Geophys. Res.,* 94:15437–15462.

Peirce, J.W., 1976. Assessing the reliability of DSDP paleolatitudes. *J. Geophys. Res.,* 81:4173–4187.

Petronotis, K.E., and Gordon, R.G., 1999. A Maastrichtian palaeomagnetic pole for the Pacific plate from a skewness analysis of marine magnetic anomaly 32. *Geophys. J. Int.,* 139:227–247.

Petronotis, K.E., Gordon, R.G., and Acton, G.D., 1992. Determining palaeomagnetic poles and anomalous skewness from marine magnetic anomaly skewness data from a single plate. *Geophys. J. Int.,* 109:209–224.

————, 1994. A 57 Ma Pacific plate paleomagnetic pole determined from a skewness analysis of crossings of marine magnetic anomaly 25r. *Geophys. J. Int.,* 118:529–554.

Roberts, A.P., Stoner, J.S., and Richter, C., 1996. Coring-induced magnetic overprints and limitations of the long-core paleomagnetic measurement technique: some observations from Leg 160, eastern Mediterranean Sea. *In* Emeis, K.-C., Robertson, A.H.F., Richter, C., et al., *Proc. ODP, Init. Repts.,* 160: College Station, TX (Ocean Drilling Program), 497–505.

Sager, W.W., 2002. Basalt core paleomagnetic data from Detroit Seamount, Northern Emperor Seamount Chain, and implications for the paleolatitude of the Hawaiian hotspot. *Earth Planet. Sci. Lett.,* 199:347–358.

Sager, W.W., Duncan, R.A., and Handschumacher, D.W., 1993. Paleomagnetism of the Japanese and Marcus-Wake seamounts, Western Pacific Ocean. *In* Pringle, M.S., Sager, W.W., Sliter, W.V., and Stein, S. (Eds.), *The Mesozoic Pacific: Geology, Tectonics, and Volcanism*. Geophys. Monogr., Am. Geophys. Union, 77:401–435.

Sager, W.W., and Koppers, A.A.P., 2000. Late Cretaceous polar wander of the Pacific plate: evidence of a true polar wander event. *Science,* 287:455–459.

Sager, W.W., and Pringle, M.S., 1988. Mid-Cretaceous to early Tertiary apparent polar wander path of the Pacific plate. *J. Geophys. Res.,* 93:11753–11771.

Shipboard Scientific Party, 2001. Leg 191 summary. *In* Kanazawa, T., Sager, W.W., Escutia, C., et al., et al., *Proc. ODP, Init. Repts.,* 191: College Station TX (Ocean Drilling Program), 1–49.

Tarduno, J.A., 1990. Absolute inclination values from deep sea sediments: a reexamination of the Cretaceous Pacific record. *Geophys. Res. Lett.,* 17:101–104.

Wallick, B.P., and Steiner, M.B., 1992. Paleomagnetism of Cretaceous basalts from the East Mariana Basin, western Pacific Ocean. *In* Larson, R.L., Lancelot, Y., et al., *Proc. ODP, Sci. Results,* 129: College Station, TX (Ocean Drilling Program), 447–454.

Figure F1. Location of Site 1179 relative to Shatsky Rise and magnetic lineations in the northwest Pacific Ocean (after Nakanishi et al., 1999; Shipboard Scientific Party, 2001).

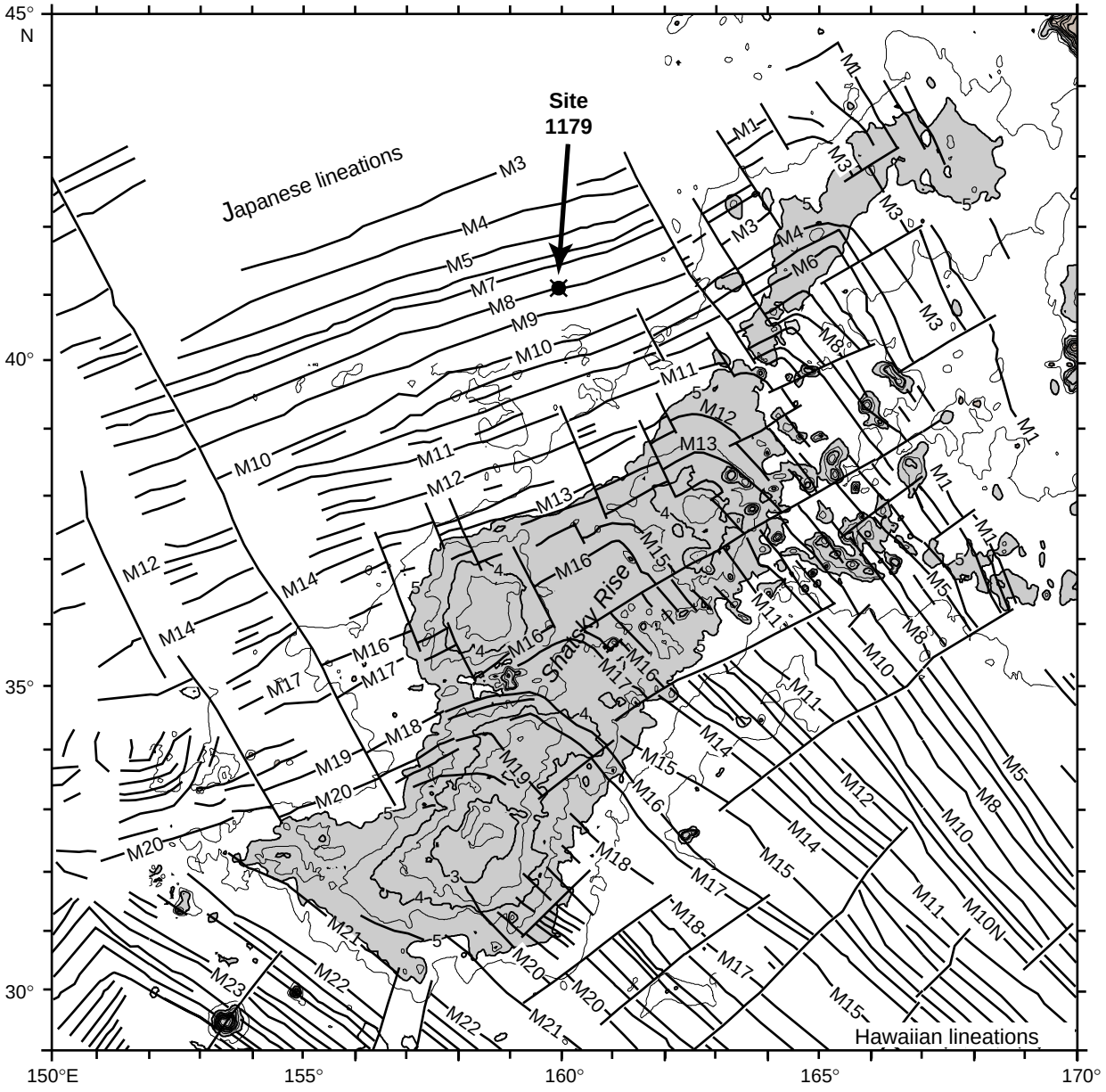

Figure F2. Orthogonal vector plots showing selected AF demagnetization experiments on Site 1179 basalt samples. Open symbols = magnetization vector endpoints projected on the vertical plane (aligned along the "up" and horizontal component, H, axes), solid symbols = points on the horizontal plane (aligned with north up and east to right). Labels give the AF field step in milliTeslas. NRM = natural remanent magnetization.

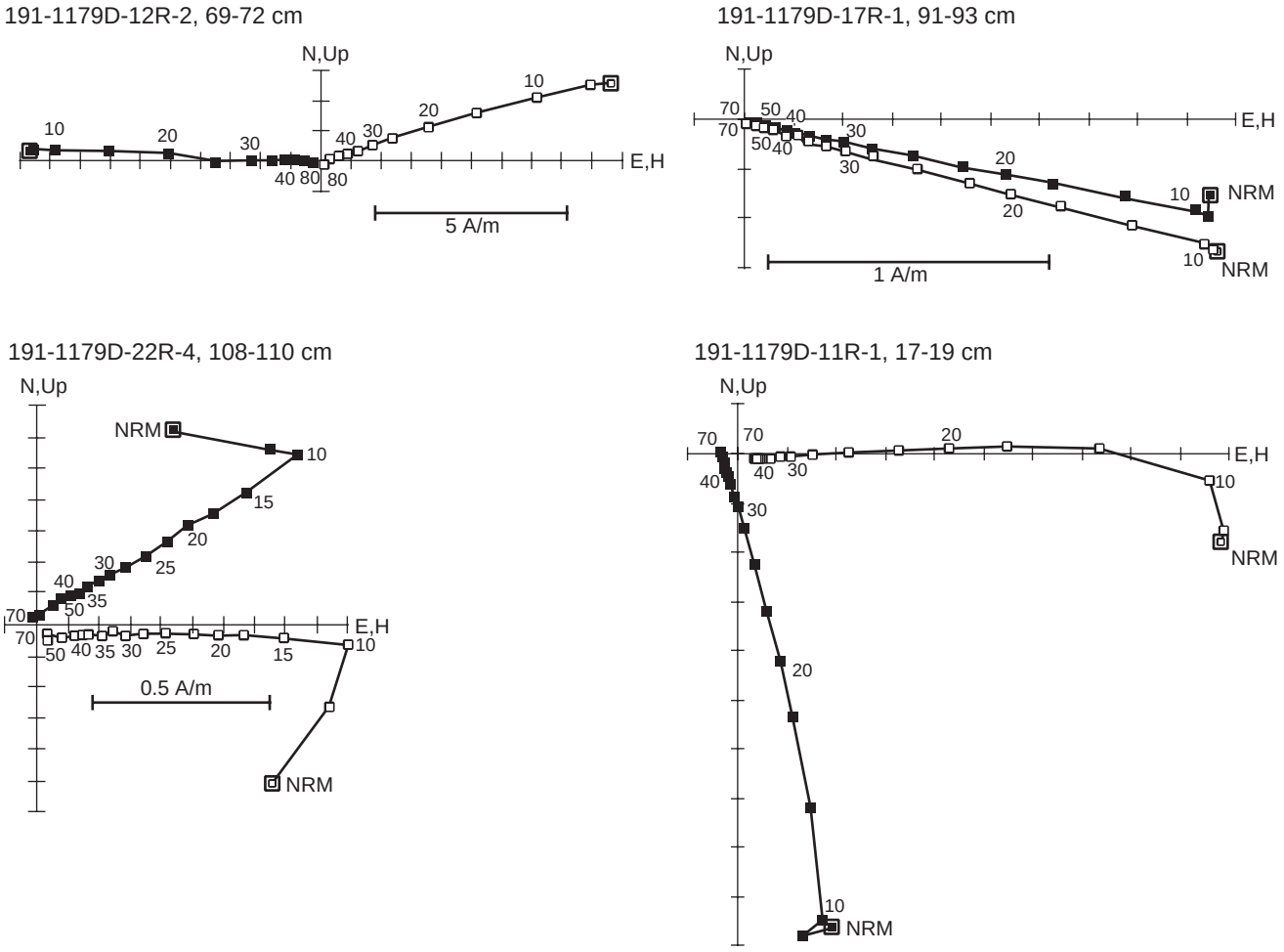

Figure F3. Orthogonal vector plots showing thermal demagnetization experiments of selected basalt samples from Site 1179. Labels give temperature steps in °C. Open symbols = magnetization vector endpoints projected on the vertical plane (aligned along the "up" and horizontal component, H, axes), and filled symbols = points on the horizontal plane (aligned with north up and east to right). NRM = natural remanent magnetization.

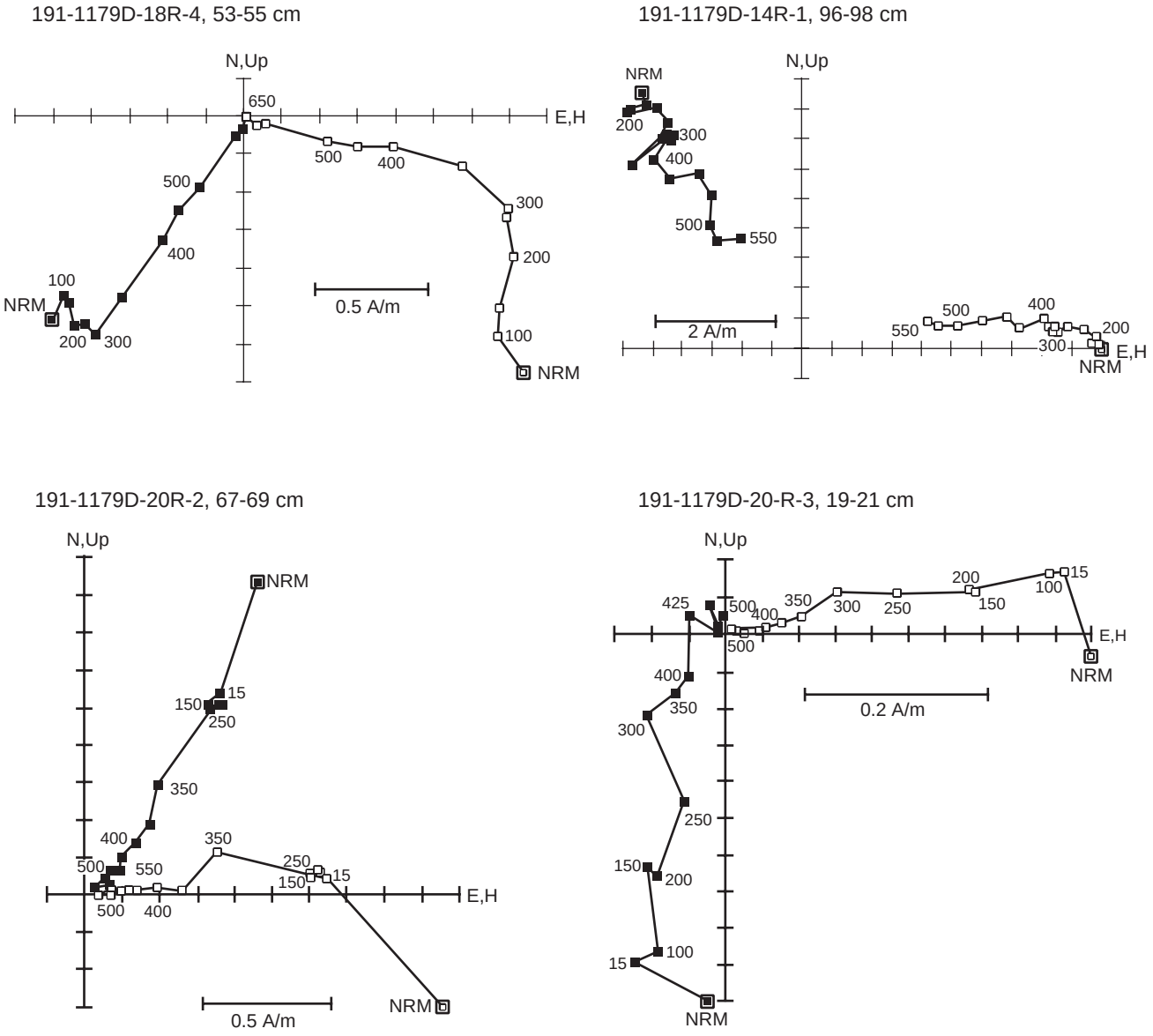

Figure F4. Measured colatitudes and flow mean colatitudes plotted vs. depth in Hole 1179D. The break in the depth column is a result of a depth curation problem that caused the bottom of one core to plot beneath the top of the next core below (see "Discussion," p. 6). Open circles = individual sample colatitude values used in the calculation of flow means, dots = sample colatitudes that were considered to be outliers and discarded from calculations, solid squares = average colatitudes for 23 statistically distinct flow groups. Horizontal lines through these symbols = the standard deviation of the flow mean colatitude, italicized numbers with each mean colatitude symbol = the flow number and number of samples used to calculate that mean (the latter in parentheses), bold red numbers give the flow groupings considered to represent independent magnetic units (Table T2). Blue shaded areas show colatitudes that were averaged in computing the 13 independent units. The red vertical dotted line shows the calculated mean site colatitude.

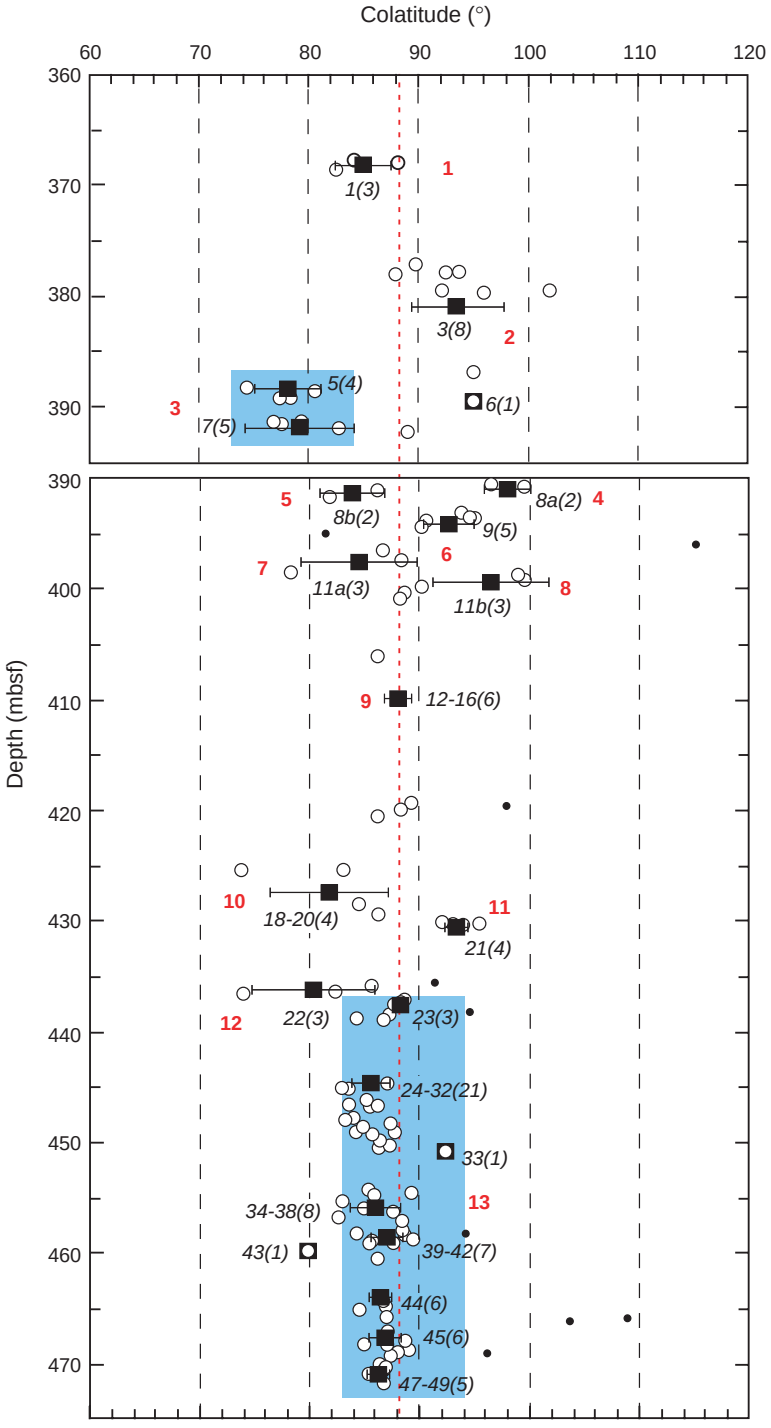

Figure F5. Comparison of Site 1179 paleocolatitude with other Pacific paleomagnetic data from basalt cores and anomalous skewness data. Heavy red arc shows the Site 1179 paleocolatitude curve (the locus of points where the paleocolatitude predicts the paleomagnetic pole to be located), assuming the section is reversed polarity (preferred model, see text for discussion), and the dashed red line shows the circle corresponding to normal polarity. Lighter arcs show paleocolatitude arcs for basalt core data from other mid-Cretaceous DSDP and ODP holes (110–130 Ma). Numbers are site numbers. Data sources are: Site 166 (Cox and Gordon, 1984); Site 289 (Hammond et al., 1975); Sites 303 and 304 (Larson and Lowrie, 1975); Sites 800 and 802 (Wallick and Steiner, 1992); Site 843 (Helsley, 1993); Site 865 (**Sager,** this volume); Sites 872, 878 (2), 879 (Nakanishi and Gee, 1995). Solid circle represents a 125-Ma paleomagnetic pole determined mainly from magnetic anomaly skewness (Petronotis et al., 1992). Solid square is a 117-Ma paleomagnetic pole calculated from averaging seamount paleomagnetic poles (Sager and Koppers, 2000). The ellipse and circle surrounding these poles are 95% confidence regions.

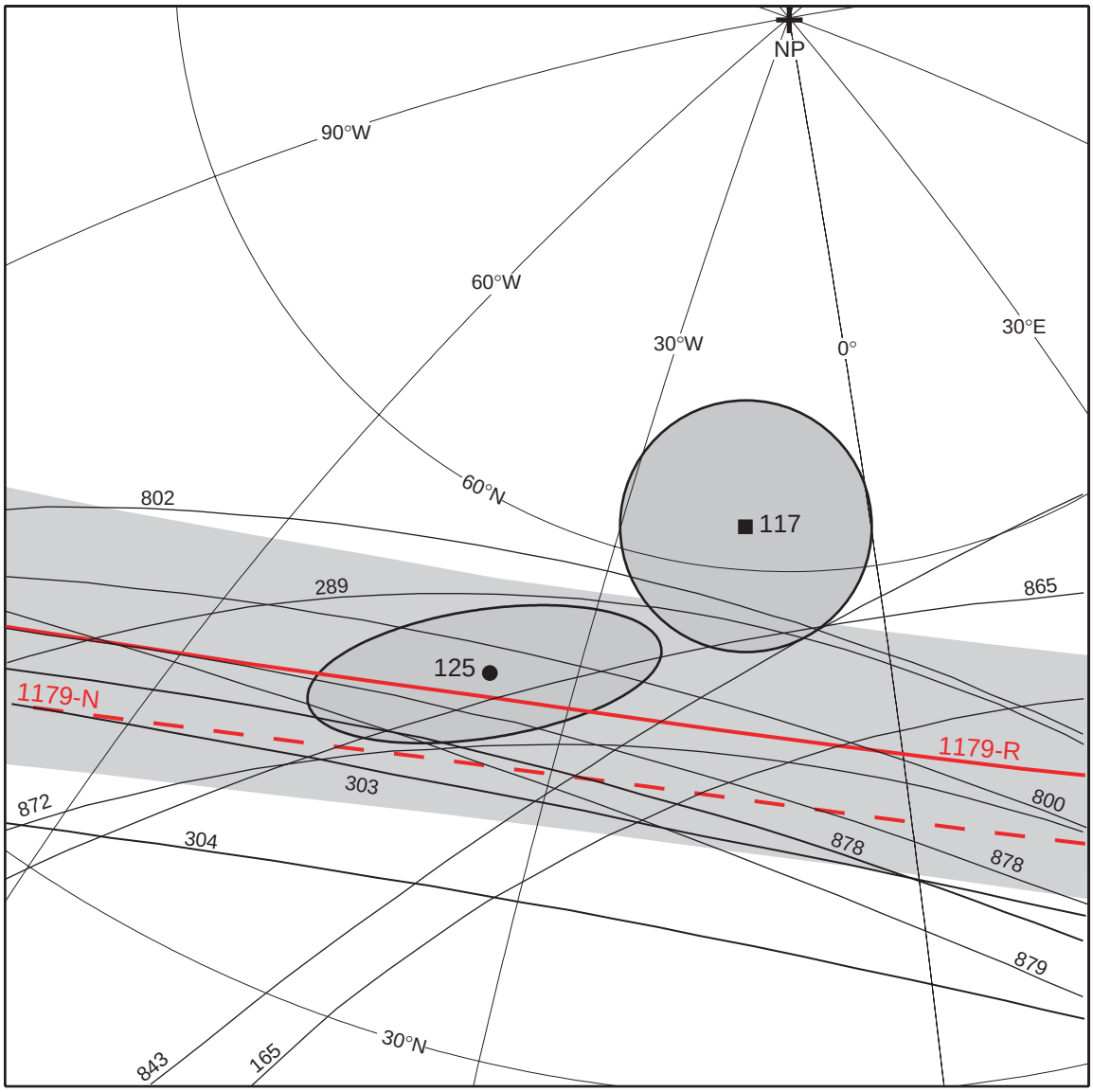

Table T1. Basalt sample paleomagnetic data, Site 1179. (See table notes. Continued on next page.)

Core, section, interval (cm)	Depth (mbsf)	Inclination (°)	Demagnetization type	*N*	Steps	MAD (°)	Lava flow	Magnetic unit	Colatitude (°)
188-1179D-									
10R-1, 53	368.03	–4	T	5	250–400	1.5	1	1	88.0
10R-1, 64	368.14	–10.3	T	4	200–350	3.6	1	1	84.8
10R-1, 102	368.52	–14.6	T	9	250–500	8.4	1	1	82.6
11R-1, 17	377.27	–0.6	A	4	15–22	1.3	3	2	89.7
11R-1, 64	377.74	7.4	A	5	20–30	1.4	3	2	93.7
11R-1, 86	377.96	–4.3	A	4	15–30	1.7	3	2	87.9
11R-1, 109	378.19	4.8	T	6	100–375	6.1	3	2	92.5
11R-2, 84	379.44	4.3	A	6	15–40	0.2	3	2	92.2
11R-2, 98	379.58	22.6	T	4	350–550	8	3	2	101.8
11R-2, 128	379.88	11.9	T	6	225–375	15.9	3	2	96.0
12R-1, 27	386.97	9.7†	T	5	350–450	11.5	3	2	94.9
12R-2, 38	388.58	–29.4	T	7	400–550	2.6	5	3	74.3
12R-2, 69	388.89	–18	A	6	25–50	1.1	5	3	80.8
12R-2, 112	389.32	–24.1†	T	5	400–500	5	5	3	77.4
12R-2, 120	389.40	–22.3	T	5	425–525	11.3	5	3	78.4
12R-2, 140	389.60	9.7	T	9	300–525	8.7	6	—	94.9*
12R-3, 81	390.51	–23.8	T	6	400–525	3.5	7	3	77.6
12R-4, 29	391.49	–24.7	T	5	300–425	15.3	7	3	77.1
12R-4, 45	391.65	–21	T	4	350–475	11.1	7	3	79.1
12R-4, 79	391.99	–14.9	A	8	15–50	2.4	7	3	82.4
12R-4, 109	392.29	–1.8†	T	5	250–400	10.8	7	3	89.1
12R-5, 14	392.84	52.7	T	5	400–500	10.3	8	—	123.3*
13R-1, 12	390.52	13.5	T	10	200–500	2.4	8a	4	96.8
13R-1, 59	390.99	19.1	T	9	350–550	13.5	8a	4	99.8
13R-1, 80	391.20	–7.2	T	7	375–525	12.6	8b	5	86.4
13R-1, 134	391.74	–15.7	T	4	400–475	12.9	8b	5	82.0
13R-2, 110	393.00	8	A	4	15–30	0.7	9	6	94.0
13R-2, 112	393.02	9.2	T	5	250–550	8	9	6	94.6
13R-2, 140	393.30	9.5	T	6	250–375	21	9	6	94.8
13R-3, 68	394.08	1.5	T	8	250–475	11.1	9	6	90.8
13R-3, 87	394.27	0.6	T	6	300–450	19	9	6	90.3
13R-4, 24	395.14	–16.6	T	6	400–550	11.8	9	—	81.5*
13R-4, 107	395.97	43.4	T	8	375–550	29.6	9	—	115.3*
14R-1, 24	396.64	–6	A	6	10–35	1.1	11a	7	87.0
14R-1, 96	397.36	–3.2	T	5	400–500	21.1	11a	7	88.4
14R-2, 77	398.67	–22.4	A	5	15–40	2.1	11a	7	78.4
14R-2, 99	398.89	18.1	T	6	350–600	10	11b	8	99.3
14R-2, 125	399.15	18.9	T	7	200–450	27.2	11b	8	99.7
14R-3, 45	399.85	0.9	T	6	250–450	21	11b	8	90.5
14R-3, 96	400.36	–2.6	T	4	475–550	21.6	12	9	88.7
14R-3, 139	400.79	–2.9	T	7	350–500	17.4	12	9	88.6
15R-1, 5	406.05	–7.4	T	7	300–500	36.2	13	9	86.3
17R-1, 53	419.33	–1.3	A	5	30–50	0.4	15	9	89.4
17R-1, 91	419.71	15.7	A	8	30–60	0.5	15	—	98.0*
17R-1, 123	420.03	–2.8	T	6	375–500	6.2	16	9	88.6
17R-2, 19	420.49	–7.4	T	5	200–375	3.9	16	9	86.3
18R-1, 10	425.40	–30	T	4	300–400	18	18	10	73.9
18R-1, 16	425.46	–13.4	T	7	250–450	19.9	18	10	83.2
18R-3, 32	428.62	–10.3	T	5	200–400	4.2	20	10	84.8
18R-3, 65	428.95	11.3	A	5	22–32	1.5	20	—	95.7*
18R-3, 113	429.43	–7.5	T	5	200–375	4.7	20	10	86.2
18R-4, 33	430.13	4.6	A	5	30–50	5	21	11	92.3
18R-4, 53	430.33	10.9	T	5	400–600	3.6	21	11	95.5
18R-4, 64	430.44	6.7	T	5	425–525	16	21	11	93.4
18R-4, 108	430.88	6.5	T	6	375–450	10.5	21	11	93.3
19R-1, 80	435.70	2.9	T	5	400–500	4.7	22	—	91.5*
19R-1, 104	435.94	–8.4	T	5	250–400	6	22	12	85.8
19R-2, 2	436.42	–14.8	T	5	400–525	6.5	22	12	82.5
19R-2, 19	436.59	–29.9	T	6	375–500	9.2	22	12	73.9
19R-2, 97	437.37	–2.6	T	5	200–375	3	23	13	88.7
19R-2, 116	437.56	–3.6	T	6	375–525	10.8	23	13	88.2
19R-2, 13	436.53	–4.4	T	7	350–500	3	23	13	87.8
19R-3, 38	438.28	9.1	T	6	350–475	10.8	24	—	94.6*
19R-3, 65	438.55	–5.7	T	6	300–450	5	24	13	87.1
19R-3, 97	438.87	–11	A	4	15–30	2	24	13	84.5
19R-3, 99	438.89	–6	T	5	350–550	1.2	24	13	87.0
20R-1, 10	444.70	–5.8	T	6	350–475	7.3	25	13	87.1

Table T1 (continued).

Core, section, interval (cm)	Depth (mbsf)	Inclination (°)	Demagnetization type	*N*	Steps	MAD (°)	Lava flow	Magnetic unit	Colatitude (°)
20R-1, 32	444.92	–13.9	T	6	375–500	3	25	13	83.0
20R-1, 53	445.13	–13.2	T	6	400–525	16.4	25	13	83.3
20R-2, 3	446.13	–9.4	T	7	350–500	3.9	26	13	85.3
20R-2, 34	446.44	–12.2	T	4	300–400	1.6	26	13	83.8
20R-2, 55	446.65	–6.8	T	4	300–400	1.7	26	13	86.7
20R-2, 67	446.77	–7.6	T	5	400–500	8.7	27	13	86.2
20R-3, 19	447.79	–12.9	T	4	250–375	20.1	29	13	83.5
20R-3, 34	447.94	–11.8	T	5	450–550	8.2	29	13	84.0
20R-3, 58	448.18	–5.2	A	8	32–70	3.6	29	13	87.4
20R-3, 96	448.56	–10.7	T	6	375–500	7.2	29	13	84.6
20R-3, 112	448.72	–10.2	T	4	300–400	2.1	30	13	84.9
20R-3, 132	448.92	–10.9	T	4	250–375	8.4	30	13	84.5
20R-4, 2	449.12	–4.2	T	7	350–500	4.6	30	13	87.9
20R-4, 39	449.49	–7.2	T	4	300–400	6.7	31	13	86.4
20R-4, 92	450.02	–6.5	T	6	250–500	3.6	31	13	86.7
20R-4, 114	450.24	–5.7	T	6	350–475	13.2	32	13	87.1
20R-4, 131	450.41	–6.6	T	6	350–475	4	32	13	86.7
20R-5, 20	450.80	5	T	8	375–550	4.4	33	13	92.5*
21R-1, 14	454.34	–8.4	T	8	300–500	4.3	34	13	85.8
21R-1, 26	454.46	–1.1	T	3	200–300	1.8	34	13	89.5
21R-1, 63	454.83	–8.1	T	7	350–475	5	35	13	85.9
21R-1, 107	455.27	–13.4	T	5	350–450	10	36	13	83.2
21R-2, 12	455.82	–10	T	5	375–500	5.6	36	13	85.0
21R-2, 54	456.24	–4.3	A	7	35–70	1.3	37	13	87.9
21R-2, 118	456.88	–14	T	6	375–500	5.7	38	13	82.9
21R-3, 13	457.33	–3.2	A	5	20–40	0.7	38	13	88.4
21R-3, 52	457.72	–3.3	T	5	250–400	6.4	39	13	88.5
21R-3, 74	457.94	–3	T	4	375–450	3.3	40	13	88.5
21R-3, 115	458.35	–2.5†	T	6	300–450	1.8	40	13	88.8
21R-3, 133	458.53	–11.3	T	6	400–525	10.8	41	13	84.3
21R-4, 2	458.72	–1.8	A	4	20–35	2	41	13	89.1
21R-4, 21	458.91	–7.8	T	5	350–550	1.1	41	13	86.1
21R-4, 37	459.07	–6.9	T	4	350–425	4.9	41	13	86.5
21R-4, 70	459.40	–4.4	T	5	350–475	6	42	13	87.8
21R-4, 107	459.77	–19.3	T	5	375–500	9	43	13	80.1*
21R-5, 24	460.44	–7.4	T	5	250–400	2.3	44	13	86.3
22R-1, 47	464.27	–6.1	T	6	325–500	2.2	44	13	86.9
22R-1, 68	464.48	–6.2	T	6	400–550	7.5	44	13	86.9
22R-1, 110	464.90	–10.4	T	6	375–500	6.3	44	13	84.8
22R-2, 18	465.48	–5.3	T	5	350–450	2.7	44	13	87.3
22R-2, 66	465.96	34.5	T	9	350–550	8.2	44	—	109.0*
22R-2, 84	466.14	26	T	6	350–475	3.1	44	—	103.7*
22R-3, 8	466.88	–5.3	T	4	350–425	3.5	44	13	87.3
22R-3, 122	468.02	–2.3	T	5	400–525	17.6	45	13	88.9
22R-3, 136	468.16	–9.6	T	5	350–450	6.5	45	13	85.2
22R-4, 7	468.37	–5.3	A	5	25–40	1.3	45	13	87.3
22R-4, 9	468.39	–2.1	T	4	350–500	1.6	45	13	89.0
22R-4, 44	468.74	–3.8	T	5	350–475	1.6	45	13	88.1
22R-4, 64	468.94	12.5	T	5	350–525	9.9	45	—	96.3*
22R-4, 108	469.38	–4.9	A	6	32–50	4.1	45	13	87.6
22R-5, 26	470.06	–6.6	T	8	300–500	2.6	47	13	86.7
22R-5, 41	470.21	–6.5	A	5	30–50	0.9	47	13	86.7
22R-5, 71	470.51	–6.5	T	5	350–400	12.3	47	13	86.7
22R-5, 103	470.83	–8.7	T	6	150–400	6.4	47	13	85.6
22R-6, 21	471.51	–5.9	T	4	425–500	2.9	48	13	87.0

Notes: Inclination of characteristic remanent magnetization was determined by principal component analysis. T = thermal, A = alternating field. *N* = number of measurements used for principal component analysis. MAD = maximum angle of deviation (Kirshvink, 1980). Lava flows are from Shipboard Scientific Party, 2001. * = colatitude not used in paleolatitude calculations. † = principal component analysis used anchor point at origin. — = not applicable.

Table T2. Paleomagnetic unit averaging results, Site 1179.

Group	Lava flow	Colatitude (°)	Standard Deviation (°)	*N*
1	1	85.1	3.72	3
2	3	93.6	4.26	8
3	5, 7	78.4	3.81	9
4	8a	98.3	2.11	2
5	8b	84.2	3.10	2
6	9	92.9	2.19	5
7	11a	84.6	5.44	3
8	11b	96.5	5.23	3
9	12–16	88.0	1.33	6
10	18, 20	82.0	5.56	4
11	21	93.6	1.35	4
12	22	80.7	6.10	3
13	23–49	86.8	1.42	57

Note: *N* = number of samples.

Table T3. Mean colatitude statistics.

Statistic	Value (°)
Mean sample variance	14.6
Mean colatitude (corrected)	88.1
Standard deviation of colatitude	6.1
Between flow variance	4.8
Systematic error	2
Random error	2.7
Standard error of mean colatitude	3.4

Note: Statistical parameter definitions given in Cox and Gordon (1984).